

# Inversion of Circularly Polarized Luminescence in Phenylethynyl-substituted Binaphthol Derivatives

Ayumi Imayoshi,<sup>\*1</sup> Shinya Fujio,<sup>1</sup> Yuuki Nagaya,<sup>1</sup> Misato Sakai,<sup>1</sup> Atsushi Terazawa,<sup>1</sup> Misa Sakura,<sup>1</sup> Keita Okada,<sup>2</sup> Takahiro Kimoto,<sup>2</sup> Tadashi Mori,<sup>3</sup> Yoshitane Imai,<sup>2</sup> Masahiko Hada,<sup>1</sup> Kazunori Tsubaki<sup>\*1</sup>

<sup>1</sup>Graduate School of Life and Environmental Sciences, Kyoto Prefectural University, 1-5 Hangi-cho, Shimogamo, Sakyo-ku, Kyoto 606-8522, Japan

<sup>2</sup>Department of Applied Chemistry, Faculty of Science and Engineering, Kindai University, 3-4-1 Kowakae, Higashi-Osaka, Osaka 577-8502, Japan

<sup>3</sup>Department of Applied Chemistry, Graduate School of Engineering, Osaka University, 2-1 Yamada-oka, Suita, Osaka 565-0871, Japan

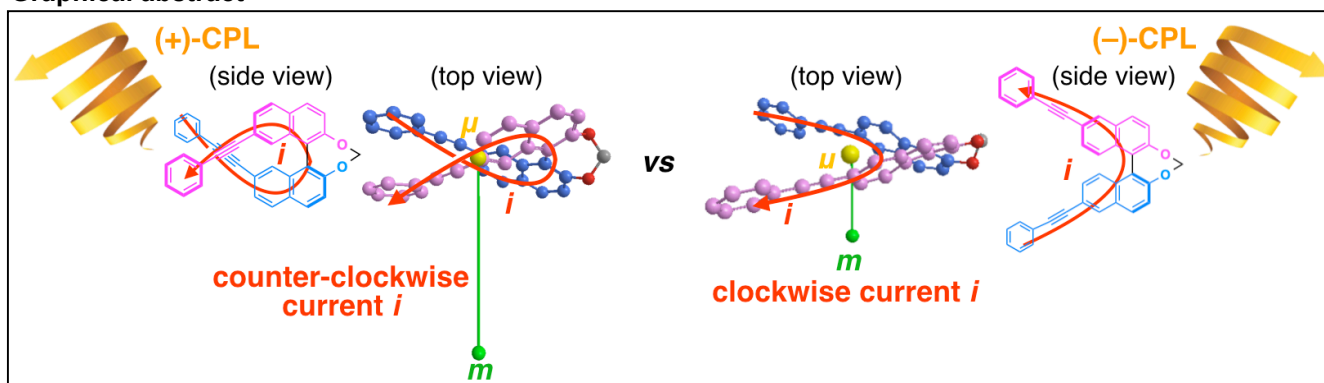
\*Corresponding author: Graduate School of Life and Environmental Sciences, Kyoto Prefectural University, 1-5 Hangi-cho, Shimogamo, Sakyo-ku, Kyoto 606-8522, Japan. Email: imayoshi@kpu.ac.jp; tsubaki@kpu.ac.jp

## Abstract

An inversion in the sign of circularly polarized luminescence (CPL) was achieved by strategically varying the substitution positions of phenylethynyl (PE) groups on the binaphthyl backbone while maintaining consistent axial chirality. Theoretical investigations indicated that the substitution position of PE groups on binaphthyl significantly influence the orientation of the transition dipole moments in the excited state, resulting in the sign inversion of CPL in **7-PE<sub>n</sub>** compared with other substrates.

**Keywords:** magnetic dipole moment, electric current, binaphthyl

## Graphical abstract



1 Circularly polarized luminescence (CPL) has  
2 attracted significant interest in recent years owing to,  
3 alongside its potential applications,<sup>01</sup> its ability to  
4 provide insights into the structure-property relationship  
5 of molecules in their excited states. The binaphthyl  
6 motif has emerged as a prominent scaffold for  
7 integrating chiral elements, and numerous chiral  
8 binaphthyl derivatives exhibiting robust CPL have  
9 been documented,<sup>02</sup> including its uses as additives,<sup>03</sup>  
10 ligands<sup>04</sup> and polymers<sup>05</sup>.

11 Theoretically, the sign of CPL is expected to  
12 reverse upon the introduction of a chiral element with  
13 an opposite configuration. However, binaphthyls with  
14 identical axial handedness can also invert their  
15 chiroptical properties, depending on factors such as

compound	$g_{lum}$ (exp)
(S)- <b>3-PE<sub>1</sub></b>	$-1.5 \times 10^{-3}$
(S)- <b>4-PE<sub>1</sub></b>	$-0.52 \times 10^{-3}$
(S)- <b>5-PE<sub>1</sub></b>	$-1.9 \times 10^{-3}$
(S)- <b>6-PE<sub>1</sub></b>	$-1.8 \times 10^{-3}$
(S)- <b>7-PE<sub>1</sub></b>	$+5.6 \times 10^{-3}$
(S)- <b>8-PE<sub>1</sub></b>	$-1.8 \times 10^{-3}$

**Figure 1.** Summary of our recent study<sup>11</sup> on methylene-linked binaphthol derivatives (S)-**3-PE<sub>1</sub>** to (S)-**8-PE<sub>1</sub>** with phenylethynyl (PE) groups at from 3,3' to 8,8' positions on the binaphthyl backbone and their dissymmetry ( $g_{lum}$ ) values for CPL.

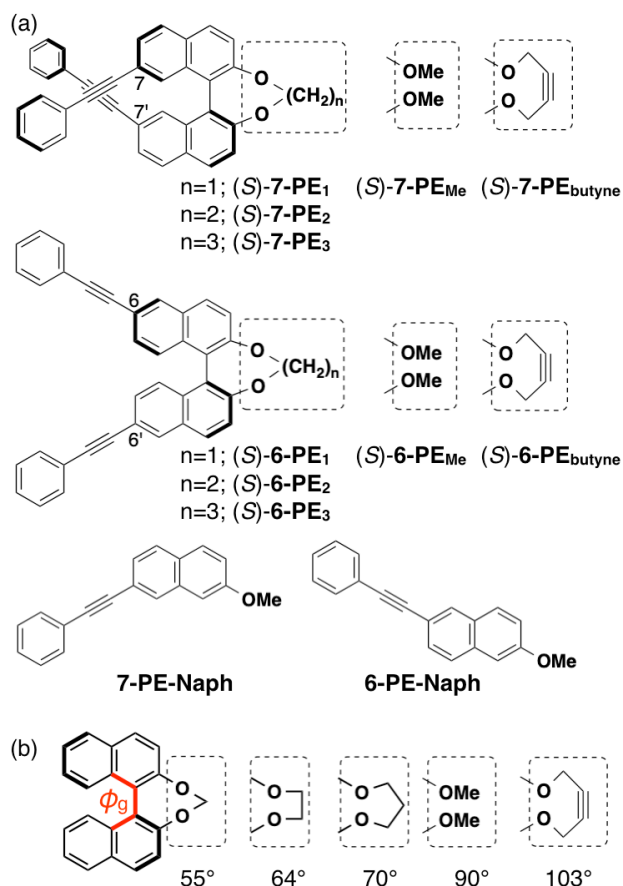


**Figure 2.** (a) Structures of binaphthol derivatives **7-PE<sub>n</sub>** and **6-PE<sub>n</sub>**, along with their naphthalene (Naph) units. (b) Variation of dihedral angles between naphthalene rings in the ground state ( $\phi_g$ ) calculated at the B3LYP/6-31G(d,p) level.

1 the dihedral angle ( $\phi$ ) between the binaphthyl units or  
 2 the structure of the linker in the binaphthol's hydroxy  
 3 groups.<sup>06</sup> Takaishi and Ema *et al.* demonstrated  
 4 through computational investigations that the CPL sign  
 5 of (*S*)-1,1'-binaphthyl reverses at a dihedral angle of  
 6 around 90°.<sup>07</sup>

7 The sign of CPL can be inverted not only through  
 8 structural modifications<sup>08,2f,2g</sup> but also by varying the  
 9 environmental conditions of the molecule,<sup>09</sup> such as  
 10 solvent<sup>10,2b</sup> and temperature.<sup>2d,3c</sup> This inversion occurs  
 11 while maintaining the same handedness in the  
 12 binaphthyl core. However, a deeper understanding of  
 13 the relationship between these chemical structures  
 14 and the CPL sign remains elusive, particularly  
 15 regarding the electronic ( $\mu$ ) and magnetic ( $m$ )  
 16 transition dipole moments crucial for enhancing the  
 17 dissymmetry ( $g_{lum}$ ) value. This value is defined as  $2(I_L$   
 18  $- I_R) / (I_L + I_R)$ , where  $I_L$  and  $I_R$  represent the intensity of  
 19 left and right-handed CPL, respectively.

20 Recently, we reported a complete series of  
 21 binaphthyl derivatives with a methylene tether,  
 22 incorporating phenylethynyl (PE) groups at the 3,3'- to  
 23 8,8'-positions of a 1,1'-bi-2-naphthol backbone (**3-PE<sub>1</sub>**

24 to **8-PE<sub>1</sub>**). Among these, only **7-PE<sub>1</sub>** exhibited a  
 25 reversal in the CPL sign (Figure 1).<sup>11</sup>

26 In this study, we performed further CPL studies on  
 27 binaphthyl derivatives with varied tether groups and  
 28 PE-substitution locations. We specifically focused on  
 29 **7-PE<sub>n</sub>** and **6-PE<sub>n</sub>**, which exhibit positive and negative  
 30 CPL, respectively, to elucidate the details behind these  
 31 observations. The binaphthol derivatives **7-PE<sub>n</sub>** and **6-PE<sub>n</sub>**  
 32 feature free methoxy groups ( $n = \text{Me}$ ) or are  
 33 connected by methylene, ethylene, and propylene  
 34 chains ( $n = 1, 2, \text{ or } 3$ , represented as  $-(\text{CH}_2)_n-$  along  
 35 with a  $-\text{CH}_2\text{C}\equiv\text{CCH}_2-$  linker ( $n = \text{butyne}$ ) (Figure 2a).  
 36 This systematic alteration affects the dihedral angle  
 37 between the naphthalenes (**7-PE-Naph** and **6-PE-**  
 38 **Naph**) in their ground ( $\phi_g$ ) and excited ( $\phi_{ex}$ ) states. The  
 39 former was promptly confirmed by density functional  
 40 theory (DFT) calculations at the B3LYP/6-31G(d,p)  
 41 level (Figure 2b).

42 Figure 3a–d shows the fluorescence (FL) and CPL  
 43 spectra of **7-PE<sub>n</sub>** and **6-PE<sub>n</sub>** in chloroform. To ensure  
 44 clarity, axial chirality throughout this study consistently  
 45 refers to the (*S*)-configuration for both **7-PE<sub>n</sub>** and **6-**  
 46 **PE<sub>n</sub>**. Among the derivatives of **7-PE<sub>n</sub>** and **6-PE<sub>n</sub>** ( $n = 1,$   
 47  $2, 3, \text{ Me, and butyne}$ ), the methylene-tethered  
 48 binaphthyls **7-PE<sub>1</sub>** and **6-PE<sub>1</sub>**, featuring the smallest  
 49 dihedral angles, exhibit distinct fluorescence behavior  
 50 characterized by low-energy and broad emissions at  
 51  $\lambda_{max} = 407$  and 398 nm, respectively. Both the CPL  
 52 signals of **7-PE<sub>1</sub>** and **6-PE<sub>1</sub>** have higher intensities  
 53 compared with derivatives having other linker  
 54 groups,<sup>12</sup> with substantial  $g_{lum}$  values of  $+5.6 \times 10^{-3}$   
 55 and  $-1.8 \times 10^{-3}$ , respectively. The **7-PE<sub>n</sub>** series tends  
 56 to consistently exhibit higher  $g_{lum}$  values compared  
 57 with the **6-PE<sub>n</sub>** series with identical linkers,<sup>13</sup> as  
 58 depicted in Figure 3e. Interestingly, the  $g_{lum}$  values for  
 59 **7-PE<sub>n</sub>** are more affected by the linker groups, while **6-**  
 60 **PE<sub>1</sub>** shows a significantly higher  $g_{lum}$  value in the **6-PE<sub>n</sub>**  
 61 series.

62 The main distinction between **7-PE<sub>n</sub>** and **6-PE<sub>n</sub>**  
 63 derivatives lies in the inherent difference in the CPL  
 64 sign, despite having the same axial chirality (compare  
 65 Figure 3a and c). Thus, all (*S*)-**7-PE<sub>n</sub>** compounds  
 66 exhibited CPL with positive (+) signs, while all (*S*)-**6-**  
 67 **PE<sub>n</sub>** compounds exhibited CPL with negative (–) signs,  
 68 regardless of their respective linker groups. In essence,  
 69 the inversion of CPL sign was achieved solely by  
 70 altering the PE-substitution positions on the binaphthyl  
 71 backbone.

72 To better understand the origin of this sign inversion,  
 73 theoretical investigations were conducted as follows:<sup>14</sup>  
 74 The chiroptical and structural computations for **7-PE<sub>1</sub>**  
 75 and **6-PE<sub>1</sub>** in their excited states were initially  
 76 performed using the TD-DFT approach. However, the  
 77 observed trends (i.e., CPL sign inversion) were not  
 78 properly reproduced. Consequently, we employed  
 79 time-dependent approximate coupled cluster  
 80 calculations at the RI-CC2/def2-TZVP level<sup>15</sup> in  
 81 subsequent investigations.

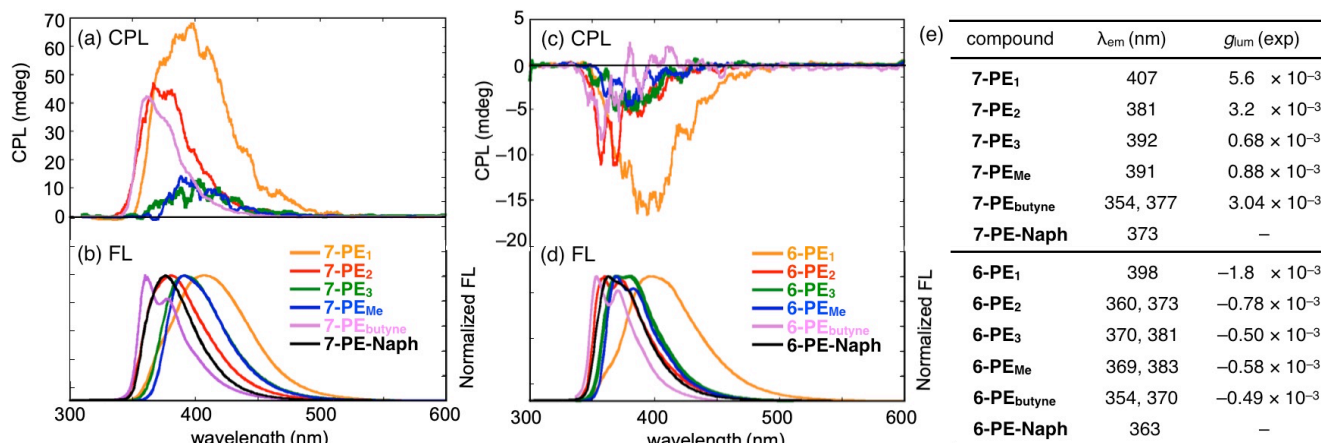


**Figure 3.** (a) CPL spectra of **7-PE<sub>n</sub>**. Conditions:  $1.0 \times 10^{-5}$  M in  $\text{CHCl}_3$ , 25 °C.  $\lambda_{ex}$  = 280 nm (**7-PE<sub>1</sub>**, **7-PE<sub>2</sub>**, **7-PE<sub>3</sub>**, **7-PE<sub>Me</sub>**), 278 nm (**7-PE<sub>butyne</sub>**). (b) FL spectra of **7-PE<sub>n</sub>** and **7-PE-Naph**. Conditions:  $1.0 \times 10^{-5}$  M in  $\text{CHCl}_3$ , 25 °C.  $\lambda_{ex}$  = 278.5 nm (**7-PE<sub>1</sub>**), 278 nm (**7-PE<sub>2</sub>**), 279 nm (**7-PE<sub>3</sub>**, **7-PE<sub>Me</sub>**), 278.5 nm (**7-PE<sub>butyne</sub>**), 278 nm (**7-PE-Naph**). (c) CPL spectra of **6-PE<sub>n</sub>**. Conditions:  $1.0 \times 10^{-5}$  M in  $\text{CHCl}_3$ , 25 °C.  $\lambda_{ex}$  = 274 nm (**6-PE<sub>1</sub>**, **6-PE<sub>2</sub>**), 277 nm (**6-PE<sub>3</sub>**), 286 nm (**6-PE<sub>Me</sub>**), 282 nm (**6-PE<sub>butyne</sub>**). (d) FL spectra of **6-PE<sub>n</sub>** and **6-PE-Naph**. Conditions:  $1.0 \times 10^{-5}$  M in  $\text{CHCl}_3$ , 25 °C.  $\lambda_{ex}$  = 284 nm (**6-PE<sub>1</sub>**, **6-PE<sub>2</sub>**), 286.5 nm (**6-PE<sub>3</sub>**), 276 nm (**6-PE<sub>Me</sub>**), 282.5 nm (**6-PE<sub>butyne</sub>**), 279 nm (**6-PE-Naph**). (e) Summary of the photophysical properties of (*S*)-**7-PE<sub>n</sub>**, **7-PE-Naph**, (*S*)-**6-PE<sub>n</sub>**, and **6-PE-Naph**.

1 Table 1 shows a comparison between the calculated  
2 and experimental  $g_{lum}$  values as derived from the  
3 optimized excited state structures. While slightly larger  
4 discrepancies were observed for **7-PE<sub>1</sub>**, the calculated  
5 values successfully reproduce the trends in both  
6 intensity and sign of the  $g_{lum}$  value.

7 Crucial structural features relevant to the electronic  
8 transitions are also summarized in Table 1. The  
9 dihedral angles between the binaphthyl units are lower  
10 in the excited state ( $\phi_{ex}$ ) compared with the ground  
11 state ( $\phi_g$ ). This structural adjustment renders the  
12 binaphthyl moieties more planar in the excited state,  
13 facilitating enhanced interaction between the  
14 naphthalene groups compared with that in the ground  
15 state.

16 The theoretical calculations also assessed the  
17 electric ( $\mu$ ) and magnetic ( $m$ ) transition dipole  
18 moments in the excited state, relevant for the  $g_{lum}$   
19 values, approximately derived for isotropic solutions as  
20  $4 (|\mu| |m| \cos\theta_{\mu m}) / (|\mu|^2 + |m|^2)$ , where  $\theta_{\mu m}$  represents

21 the angle between  $\mu$  and  $m$ . The angles  $\theta_{\mu m}$  for **7-PE<sub>1</sub>**  
22 and **6-PE<sub>1</sub>** deviated by 9.5° less and 7.8° more than  
23 90°, respectively. Thus, the deviation from a right  
24 angle was primarily responsible for the reversal in CPL  
25 sign between **7-PE<sub>n</sub>** and **6-PE<sub>n</sub>**.

26 To further understand why the orientation of  $\theta_{\mu m}$   
27 varies dramatically—spanning a right angle—between  
28 **7-PE<sub>1</sub>** and **6-PE<sub>1</sub>**, we examine in detail the relationship  
29 between molecular structures and the orientations of  $\mu$   
30 and  $m$  (see Figures 4 and 5). During the  $S_1 \rightarrow S_0$   
31 transition, when electrons move from the upper to the  
32 lower **PE-Naph** unit,  $\mu$  is directed upwards, indicating  
33 the opposite direction to the electron movement  
34 (Figures 4b and 5b). In a classical explanation, the  
35 generated current flows in the opposite direction to the  
36 electron movement. Thus, it is expected that the  
37 instantaneous current ( $i$ )<sup>16</sup> generated by  $\mu$  during an  
38 electron transition in these molecular systems will flow  
39 along  $\mu$  (from the lower to upper **PE-Naph** units), as  
40 indicated by the red arrows in Figures 4a and 5a.

41  
42  
43

**Table 1.** Characteristic features relevant to the electronic transition from the excited to the ground state ( $S_1 \rightarrow S_0$ ) calculated at the RI-CC2/def2-TZVP level

Compound	$\phi_g$ (°)	$\phi_{ex}$ (°)	$\mu$ (D)	$m$ (MB)	$\theta_{\mu m}$ (°)	$g_{lum}$ (calc)	$g_{lum}$ (exp)
<b>7-PE<sub>1</sub></b>	52.3	38.7	2.23	3.28	80.5	$9.0 \times 10^{-3}$	$5.6 \times 10^{-3}$
<b>6-PE<sub>1</sub></b>	53.4	33.2	4.37	1.44	97.8	$-1.7 \times 10^{-3}$	$-1.8 \times 10^{-3}$

$\phi_g$ : Dihedral angle of the binaphthyl in the ground state. Calculated at the TPSS-D4/def2-TZVP level.

$\phi_{ex}$ : Dihedral angle of the binaphthyl in the excited state.

$\mu$ : Electric transition dipole moment in the excited state.

$m$ : Magnetic transition dipole moment in the excited state.

$\theta_{\mu m}$ : Angle of vectors between  $\mu$  and  $m$ .

$g_{lum}$  (calc): Theoretically calculated  $g_{lum}$  value.

$g_{lum}$  (exp): Experimentally observed  $g_{lum}$  value.

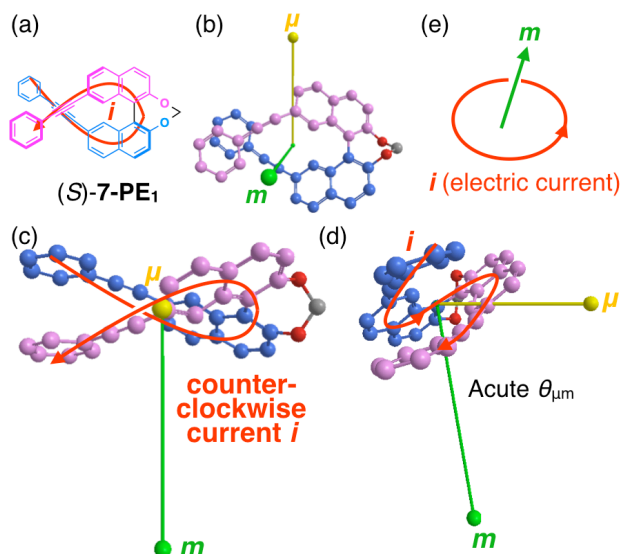


**Figure 4.** (a) Expected electric current flow ( $i$  is shown in red) for the  $S_1 \rightarrow S_0$  transitions for (S)-**7-PE**<sub>1</sub>. (b) Electric ( $\mu$  is shown in purple) and magnetic ( $m$  is shown in blue) transition dipole moments for the  $S_1 \rightarrow S_0$  transitions for (S)-**7-PE**<sub>1</sub>. For clarity, the relative length of  $m$  is magnified by 137 times compared with that of  $\mu$ . (c) Top view from the direction of  $\mu$ . The current flows counterclockwise relative to the origin- $\mu$  axis. (d) Side view from the direction of  $\mu$ . The  $\theta_{\mu m}$  is clearly acute. (e) Relationship between electric current and  $m$  according to the classic loop model.

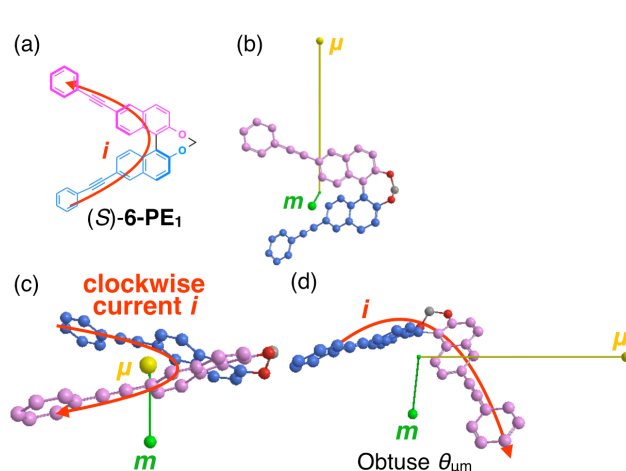


**Figure 5.** (a) Expected electric current flow ( $i$  is shown in red) for the  $S_1 \rightarrow S_0$  transitions for (S)-**6-PE**<sub>1</sub>. (b) Electric ( $\mu$  is shown in purple) and magnetic ( $m$  is shown in blue) transition dipole moments for the  $S_1 \rightarrow S_0$  transitions for (S)-**6-PE**<sub>1</sub>. For clarity, the relative length of  $m$  is magnified by 137 times compared with that of  $\mu$ . (c) Top view from the direction of  $\mu$ . The current flows clockwise relative to the origin- $\mu$  axis. (d) Side view from the direction of  $\mu$ . Note that  $\theta_{\mu m}$  is clearly obtuse.

1 Importantly, in **7-PE**<sub>1</sub>, the current flows  
 2 counterclockwise relative to the origin- $\mu$  axis (Figure  
 3 4c), and clockwise in **6-PE**<sub>1</sub> (Figure 5c). Despite similar  
 4 directions of electron movement from the upper to  
 5 lower **PE-Naph** units in both **7-PE**<sub>1</sub> and **6-PE**<sub>1</sub>, the  
 6 direction of current rotation is apparently reversed.  
 7 According to the classic loop model (Figure 4e), the  
 8 reversal in current-flow direction inversely affects the  
 9 direction of  $m$ . Consequently, this reversal in current  
 10 direction—and thus in orientation of  $m$ —between **7-PE**<sub>1</sub>  
 11 and **6-PE**<sub>1</sub> accounts for the angle  $\theta_{\mu m}$  being obtuse  
 12 in **7-PE**<sub>1</sub> and acute in **6-PE**<sub>1</sub> (Figure 4d and 5d). Thus,  
 13 **7-PE**<sub>1</sub> exhibited left-handed CPL, while **6-PE**<sub>1</sub> showed  
 14 right-handed CPL. Additionally, the more pronounced  
 15 coil-like flow of current in **7-PE**<sub>1</sub> results in a larger  $m$   
 16 and thus a higher  $g_{lum}$  value compared to that in **6-PE**<sub>1</sub>  
 17 (compare Figures 4d and 5d).

18 Our rationale may aid in understanding the  
 19 structure-property relationship of  $m$ , especially for  $C_2$ -  
 20 symmetric molecules like **7-PE**<sub>1</sub> and **6-PE**<sub>1</sub>, where the  
 21  $S_1 \rightarrow S_0$  transition mainly involves LUMO  $\rightarrow$  HOMO  
 22 transitions. Similarly, this reasoning would explain why  
 23 compounds such as **3-PE**<sub>1</sub>, **4-PE**<sub>1</sub>, **5-PE**<sub>1</sub>, and **8-PE**<sub>1</sub>  
 24 also exhibit negative CPL like **6-PE**<sub>n</sub> (see Figure S3–  
 25 S6).

26 As mentioned above, among the **6-PE**<sub>n</sub> series, the  
 27  $g_{lum}$  value of **6-PE**<sub>1</sub> exhibited a significantly higher  
 28 value, while the  $g_{lum}$  values of **7-PE**<sub>n</sub> were considerably

29 influenced by the linker groups (Figure 3e).  
 30 Interestingly, **6-PE**<sub>1</sub> has a helicene-like twisted  
 31 structure in the excited state (Figure 6c), while in the  
 32 ground state, it bears the typical binaphthyl  
 33 conformation. Indeed, the trend in the degree of  
 34 torsional angles considerably differs in these systems  
 35 ( $\phi$  and  $\phi'/\phi''$  in Figure 6a). Both **7-PE**<sub>1</sub> and **6-PE**<sub>Me</sub>  
 36 having typical binaphthyl conformations in the excited  
 37 state show angles of 39° and 9/9° or 65° and 3/3°,  
 38 respectively (Figure 6b, d). In contrast, these angles  
 39 were found to be 33° and 31/20° in **6-PE**<sub>1</sub>, resulting in  
 40 a greatly twisted conformation similar to that of a

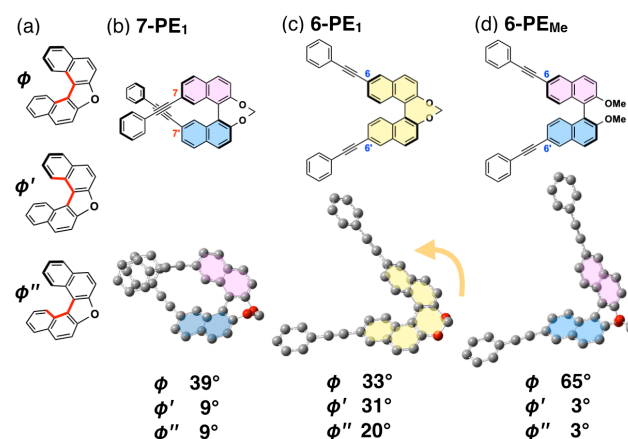


**Figure 6.** (a) Definition of torsional angles ( $\phi$ ,  $\phi'$  and  $\phi''$ ) of binaphthyls. Optimized structures in the excited state and the corresponding angles for (b) **7-PE**<sub>1</sub>, (c) **6-PE**<sub>1</sub> and (d) **6-PE**<sub>Me</sub>.

1 typical helicene structure.<sup>17</sup> This unexpected structural  
2 change in the excited state of **6-PE<sub>1</sub>** is most likely  
3 responsible for its red-shifted emission and better  $g_{lum}$   
4 value compared with the other **6-PE<sub>n</sub>** derivatives.

5 In summary, the introduction of PE groups at the  
6 6,6'- or 7,7'-positions of the (S)-binaphthyl backbone  
7 results in oppositely signed CPL responses. While the  
8 methylene-tethered **7-PE<sub>1</sub>** and **6-PE<sub>1</sub>** derivatives  
9 display superior  $g_{lum}$  values, sign inversion is uniformly  
10 observed across all related derivatives. Theoretical  
11 calculations provided a rationale for the sign inversion  
12 and other differences in chiroptical responses.

13 We anticipate that our observations and the insights  
14 derived from our detailed structural analyses of  
15 binaphthyls in the excited state will contribute to  
16 understanding other novel CPL phenomena,  
17 particularly those exhibited by binaphthyl compounds.

### 19 Acknowledgement

20 The authors are grateful to Prof. Keiji Hirose and  
21 Dr. Rika Miyake (Graduate School of Engineering  
22 Science, Osaka University), Prof. Yasunao Hattori  
23 (Center for Instrumental Analysis, Kyoto  
24 Pharmaceutical University) and Prof. Takumi Furuta  
25 (Laboratory of Pharmaceutical Chemistry, Kyoto  
26 Pharmaceutical University), and Prof. Makoto Oba and  
27 Dr. Tomohiro Umeno (Graduate School of Medicine,  
28 Kyoto Prefectural University of Medicine) for the  
29 HRMS measurements. This study was carried out  
30 using the FT-ICR mass spectrometer and the NMR  
31 spectrometer in the Joint Usage/ Research Center at  
32 the Institute for Chemical Research, Kyoto University.  
33 The computation was performed using Research  
34 Center for Computational Science, Okazaki, Japan  
35 (Project: 23-IMS-C043). We thank Dr. Jay Freeman at  
36 Edanz (<https://jp.edanz.com/ac>) for editing a draft of  
37 this manuscript.

### 40 Funding

41 This study was supported in part by Japan Society for  
42 the Promotion of Science (JSPS) KAKENHI (Nos.  
43 24K18254, 22K15256, 19K23803, 22H02746 and  
44 19H03355), Japan Science and Technology Agency  
45 (JST) CREST (JPMJCR2001), and Grant-in-Aid from  
46 the Naito Foundation.

47 *Conflict of interest statement.* None declared.  
48  
49

### 50 References

51 1 a) J. R. Brandt, F. Salerno, M. J. Fuchter, *Nature Reviews*  
52 *Chemistry* **2017**, *1*, 1. b) Y. Sang, J. Han, T. Zhao, P. Duan,  
53 M. Liu, *Adv. Mater.* **2020**, *32*, e1900110. c) Y. Deng, M.  
54 Wang, Y. Zhuang, S. Liu, W. Huang, Q. Zhao, *Light: Sci.*  
55 *Appl.* **2021**, *10*, 1. d) J. Han, S. Guo, H. Lu, S. Liu, Q. Zhao,  
56 W. Huang, *Adv. Opt. Mater.* **2018**, *6*, 1800538. e) X. Wang,  
57 S. Ma, B. Zhao, J. Deng, *Adv. Funct. Mater.* **2023**, *33*,  
58 2214364. f) Y. Yang, N. Li, J. Miao, X. Cao, A. Ying, K. Pan,  
59 X. Lv, F. Ni, Z. Huang, S. Gong, C. Yang, *Angew. Chem.*

60 *Int. Ed.* **2022**, *61*, e202202227. g) D.-W. Zhang, M. Li, C.-F.  
61 Chen, *Chem. Soc. Rev.* **2020**, *49*, 1331. h) I. Song, J. Ahn,  
62 H. Ahn, S. H. Lee, J. Mei, N. A. Kotov, J. H. Oh, *Nature*  
63 **2023**, *617*, 92. i) L. E. MacKenzie, R. Pal, *Nature Reviews*  
64 *Chemistry* **2020**, *5*, 109. j) Y. Shi, J. Han, X. Jin, W. Miao,  
65 Y. Zhang, P. Duan, *Adv. Sci.* **2022**, *9*, e2201565.  
66 2 a) Y. Nojima, M. Hasegawa, N. Hara, Y. Imai, Y. Mazaki,  
67 *Chem. Eur. J.* **2021**, *27*, 5923. b) Z.-B. Sun, J.-K. Liu, D.-F.  
68 Yuan, Z.-H. Zhao, X.-Z. Zhu, D.-H. Liu, Q. Peng, C.-H.  
69 Zhao, *Angew. Chem. Int. Ed.* **2019**, *58*, 4840. c) K. Miki, T.  
70 Noda, M. Gon, K. Tanaka, Y. Chujo, Y. Mizuhata, N.  
71 Tokitoh, K. Ohe, *Chem. Eur. J.* **2019**, *25*, 9211. d) K.  
72 Takaishi, F. Yoshinami, Y. Sato, T. Ema, *Chem. Eur. J.*  
73 **2024**, e202400866. e) K. Takaishi, S. Murakami, F.  
74 Yoshinami, T. Ema, *Angew. Chem. Int. Ed.* **2022**, *61*,  
75 e202204609. f) K. Takaishi, K. Iwachido, R. Takehana, M.  
76 Uchiyama, T. Ema, *J. Am. Chem. Soc.* **2019**, *141*, 6185. g)  
77 J. Li, C. Hou, C. Huang, S. Xu, X. Peng, Q. Qi, W.-Y. Lai,  
78 W. Huang, *Research* **2020**, *2020*, 3839160. h) W. Duan, K.  
79 Li, H. Ji, Y. Huo, Q. Yao, H. Liu, S. Gong, *Dyes Pigm.* **2021**,  
80 *193*, 109538. i) Z. Jiang, X. Wang, J. Ma, Z. Liu, *Sci. China*  
81 *Chem.* **2019**, *62*, 355. j) J. Han, Y. Shi, X. Jin, X. Yang, P.  
82 Duan, *Chem. Sci.* **2022**, *13*, 6074. k) H. Feng, J. Pu, S.  
83 Wang, S. Jiang, W. Yang, D. Cao, Y.-S. Feng, *Dyes Pigm.*  
84 **2023**, *217*, 111422. l) F. Song, Z. Xu, Q. Zhang, Z. Zhao, H.  
85 Zhang, W. Zhao, Z. Qiu, C. Qi, H. Zhang, H. H. Y. Sung, I.  
86 D. Williams, J. W. Y. Lam, Z. Zhao, A. Qin, D. Ma, B. Z.  
87 Tang, *Adv. Funct. Mater.* **2018**, *28*, 1800051. m) Y. Wang,  
88 X. Li, F. Li, W.-Y. Sun, C. Zhu, Y. Cheng, *Chem.*  
89 *Commun.* **2017**, *53*, 7505. n) Q. Ye, D. Zhu, L. Xu, X. Lu,  
90 Q. Lu, *J. Mater. Chem.* **2016**, *4*, 1497.  
91 3 a) Y. He, S. Lin, J. Guo, Q. Li, *Aggregate (Hoboken)* **2021**,  
92 *2*, e141. b) S. Yang, F. Li, Q. Li, J. Han, Y. Cheng, *ACS*  
93 *Appl. Opt. Mater.* **2023**, *1*, 1492. c) Y. Zhang, H. Li, Z.  
94 Geng, W.-H. Zheng, Y. Quan, Y. Cheng, *ACS Nano* **2022**,  
95 *16*, 3173.  
96 4 a) N. F. M. Mukthar, N. D. Schley, G. Ung, *J. Am. Chem.*  
97 *Soc.* **2022**, *144*, 6148. b) Y. Zhou, H. Li, T. Zhu, T. Gao, P.  
98 Yan, *J. Am. Chem. Soc.* **2019**, *141*, 19634.  
99 5 a) Z. Geng, Y. Zhang, Y. Zhang, Y. Li, Y. Quan, Y. Cheng,  
100 *J. Mater. Chem.* **2021**, *9*, 12141. b) Z. Geng, Y. Zhang, Y.  
101 Zhang, Y. Quan, Y. Cheng, *Angew. Chem. Int. Ed.* **2022**,  
102 *61*, e202202718.  
103 6 Y. Nojima, M. Hasegawa, N. Hara, Y. Imai, Y. Mazaki,  
104 *Chem. Commun.* **2019**, *55*, 2749. b) T. Sato, N. Tajima, H.  
105 Ueno, T. Harada, M. Fujiki, Y. Imai, *Tetrahedron* **2016**, *72*,  
106 7032. c) T. Kinuta, N. Tajima, M. Fujiki, M. Miyazawa, Y.  
107 Imai, *Tetrahedron* **2012**, *68*, 4791. d) T. Kimoto, N. Tajima,  
108 M. Fujiki, Y. Imai, *Chem. Asian J.* **2012**, *7*, 2836.  
109 7 K. Takaishi, T. Matsumoto, M. Kawataka, T. Ema, *Angew.*  
110 *Chem. Int. Ed.* **2021**, *60*, 9968.  
111 8 a) K. Takaishi, S. Murakami, K. Iwachido, T. Ema, *Chem.*  
112 *Sci.* **2021**, *12*, 14570. b) D. Kaji, S. Ikeda, K. Takamura, N.  
113 Tajima, M. Shizuma, T. Mori, M. Miyasaka, Y. Imai, *Chem.*  
114 *Lett.* **2019**, *48*, 874. c) T. Amako, T. Kimoto, N. Tajima, M.  
115 Fujiki, Y. Imai, *RSC Adv.* **2013**, *3*, 6939. d) N. Hara, D. Kaji,  
116 K. Okuda, M. Shizuma, N. Tajima, Y. Imai, *Chem. Lett.*  
117 **2018**, *47*, 894. e) K. Nakabayashi, S. Kitamura, N. Suzuki,  
118 S. Guo, M. Fujiki, Y. Imai, *Eur. J. Org. Chem.* **2016**, *2016*,  
119 64.  
120 9 a) Y. Imai, *Chem. Lett.* **2021**, *50*, 1131. b) Y. Sheng, D.  
121 Shen, W. Zhang, H. Zhang, C. Zhu, Y. Cheng, *Chem. Eur.*  
122 *J.* **2015**, *21*, 13196. c) T. Kimoto, T. Amako, N. Tajima, R.  
123 Kuroda, M. Fujiki, Y. Imai, *Asian J. Org. Chem.* **2013**, *2*,  
124 404. d) K. Nakabayashi, T. Amako, N. Tajima, M. Fujiki, Y.  
125 Imai, *Chem. Commun.* **2014**, *50*, 13228. e) Y. Li, C. Xue,  
126 M. Wang, A. Urbas, Q. Li, *Angew. Chem. Int. Ed.* **2013**, *52*,  
127 13703. f) H. Okada, N. Hara, D. Kaji, M. Shizuma, M.  
128 Fujiiki, Y. Imai, *Phys. Chem. Chem. Phys.* **2020**, *22*,  
129 13862.

- 1 10 a) K. Takaishi, K. Iwachido, T. Ema, *J. Am. Chem. Soc.*  
2 **2020**, *142*, 1774. b) S. Nakanishi, N. Hara, N. Kuroda, N.  
3 Tajima, M. Fujiki, Y. Imai, *Org. Biomol. Chem.* **2018**, *16*,  
4 1093. c) M. Okazaki, T. Mizusawa, K. Nakabayashi, M.  
5 Yamashita, N. Tajima, T. Harada, M. Fujiki, Y. Imai, *J.*  
6 *Photochem. Photobiol. A Chem.* **2016**, *331*, 115.  
7 11 M. Sakai, S. Fujio, A. Imayoshi, T. Sasamori, K. Okada, Y.  
8 Imai, M. Hasegawa, K. Tsubaki, *Chem. Asian J.* **2024**,  
9 e202400159.
- 10 12 a) K. Ma, W. Chen, T. Jiao, X. Jin, Y. Sang, D. Yang, J.  
11 Zhou, M. Liu, P. Duan, *Chem. Sci.* **2019**, *10*, 6821. b) K.  
12 Takaishi, S. Hinoide, T. Matsumoto, T. Ema, *J. Am. Chem.*  
13 *Soc.* **2019**, *141*, 11852. c) Y. Wang, Q. Liao, Y. Feng, Q.  
14 Meng, *J. Mol. Struct.* **2024**, *1304*, 137695. d) Y. Wang, Y.  
15 Li, S. Liu, F. Li, C. Zhu, S. Li, Y. Cheng, *Macromolecules*  
16 **2016**, *49*, 5444. e) T. Ikai, N. Mishima, T. Matsumoto, S.  
17 Miyoshi, K. Oki, E. Yashima, *Angew. Chem. Int. Ed.* **2024**,  
18 *63*, e202318712. f) W. Huang, Y. Zhu, K. Zhou, L. Chen, Z.  
19 Zhao, E. Zhao, Z. He, *Chem. Eur. J.* **2023**, e202303667. g)  
20 S. Jena, A. Thayyil Muhammed Munthasir, S. Pradhan, M.  
21 Kitahara, S. Seika, Y. Imai, P. Thilagar, *Chem. Eur. J.* **2023**,  
22 *29*, e202301924.
- 23 13 K. Zhang, J. Zhao, N. Zhang, J.-F. Chen, N. Wang, X. Yin,  
24 X. Zheng, P. Chen, *J. Mater. Chem.* **2022**, *10*, 1816.
- 25 14 **TURBOMOLE V7.8 2023**, a development of University of  
26 Karlsruhe and Forschungszentrum Karlsruhe GmbH, 1989-  
27 2007, *TURBOMOLE GmbH*, since **2007**; available from  
28 <https://www.turbomole.org>.
- 29 15 a) C. Hättig, A. Köhn, *J. Chem. Phys.* **2002**, *117*, 6939. b)  
30 F. Weigend, R. Ahlrichs, *Phys. Chem. Chem. Phys.* **2005**,  
31 *7*, 3297. c) F. Weigend, *Phys. Chem. Chem. Phys.* **2006**,  
32 *8*, 1057.
- 33 16 a) M. Fortino, G. Schifino, A. Pietropaolo, *Chirality* **2023**,  
34 *35*, 673. b) F. Furche, R. Ahlrichs, C. Wachsmann, E.  
35 Weber, A. Sobanski, F. Vögtle, S. Grimme, *J. Am. Chem.*  
36 *Soc.* **2000**, *122*, 1717. c) R. G. Uceda, C. M. Cruz, S.  
37 Míguez-Lago, L. Á. de Cienfuegos, G. Longhi, D. A. Pelta,  
38 P. Novoa, A. J. Mota, J. M. Cuerva, D. Miguel, *Angew.*  
39 *Chem. Int. Ed.* **2024**, *63*, e202316696.
- 40 17 P. Ravat, R. Hinkelmann, D. Steinebrunner, A. Prescimone,  
41 I. Bodoky, M. Juriček, *Org. Lett.* **2017**, *19*, 3707.